Journal Homepage: http://ijcpe.uobaghdad.edu.iq
Iraqi Journal of Chemical and Petroleum Engineering
Vol. 26 No. 3 (September 2025) 137 – 150
EISSN: 2618-0707, PISSN: 1997-4884

Improving the elimination of methyl orange dye by combining electrocoagulation system with the adsorption process by oven-dried alum sludge: adopting different combined systems

Amor T. Mohammed Ali [a], Rasha H. Salman [a, *]

a Department of Chemical Engineering, College of Engineering, University of Baghdad, Aljadria, Baghdad, Postcode: 10071, Iraq

Abstract

Due to their recalcitrant characteristics, Azo dyes such as methyl orange (MO) are extremely poisonous substances, making their removal from textile industry wastewater a major problem. By employing various EC-Adsorption combined system configurations and reusing alum sludge as an adsorbent, the current study seeks to investigate the efficiency of these various systems in removing MO dye. To estimate their benefits and limitations, experiments were carried out utilizing nickel foam (NiF) and aluminum plate (Al plate) as anodes, and stainless-steel mesh (SS mesh) as cathode in the presence of alum sludge as an adsorbent in all systems. The EC-Adsorption combined system with NiF as anode and two SS meshes as cathodes with 10 g/L of alum sludge in the solution, which is referenced as S3, offered 98.968% of MO dye removal efficiency within 30 minutes without the need for prolonged treatment and with very low concentration of leached Ni ions. The BET surface area, pore size, surface morphology, and composition of alum sludge were examined. The utilization of alum sludge in the combined system enhanced the removal of excess Ni ions and reduced its impact in the treated solutions, and moderately enhanced the MO dye removal efficiency. To attain a detailed explanation of the adsorption mechanism, various kinetics and isotherm models were applied. The adsorption of MO dye in the S3 EC-Adsorption system follows the intra-particle diffusion model, and the best-fit isotherm was the Freundlich isotherm.

Keywords: combined systems; alum sludge; electrocoagulation; Adsorption; kinetic model.

Received on 03/06/2025, Received in Revised Form on 28/06/2025, Accepted on 06/07/2025, Published on 30/09/2025

https://doi.org/10.31699/IJCPE.2025.3.12

1- Introduction

One of the most essential things for life to exist is water. However, as the world's population grows, its supplies are becoming fewer and more contaminated. Color, chemical oxygen demand (COD), and total dissolved and suspended solids are crucial elements for wastewater produced in the textile industry quality assessments [1]. The industrial sector was thought to be the main source of contamination because it generates many different kinds of pollutants [2]. One of these industries is the textile dyeing and dye making sectors, and the dye wastewater that is released into rivers, lakes, and other bodies of water are contaminated with different types of dyes which is considered a significant environmental issue that requires efficient treatment even at low concentrations. The food and cosmetics industries, as well as the paper, plastic, rubber, and leather industries, are similarly releasing large quantities of dyes and colors. A total of 700,000 tons of synthetic dyes are manufactured annually, out of 10,000 different varieties. The textile industry uses around 10,000 types of dyes and pigments, the majority of which are hazardous to both humans and aquatic life. The dyeing and coloring operations release two to five tons of dyes into the environment [3-5].

Azo dyes are one of the most widely used dyes in several industrial processes, including the production of paints, textiles, and others. Because of the way of their production, Azo dyes are quite stable in soil and water settings [6] Methyl orange (MO) is an Azo dye consumed widely in the textile industry which has a high degree of solubility in water, anionic properties, and a low degree of biodegradability. These properties of MO dye increased their toxicity and increased the necessity to remove them from effluents [7, 8].

Hence processes including dyes produce highly hazardous effluents; it is an essential step to eliminate dyes from these effluents before releasing them into aquatic water [9]. Many techniques are utilized to remove dyes from wastewater like; decomposition [10], adsorption [11], filtration, membrane [12], ion exchange [13], and coagulation-flocculation [14, 15]. The low treatment efficiency, high operational costs, or secondary pollution from deposited sludge are some of the disadvantages of these techniques [16].

Based on many previous studies, electrochemical techniques approved their capability in removing various pollutants from wastewater effectively and reducing environmental damage. Using electrochemical processes has several benefits, including cost-effectiveness, safety,

*Corresponding Author: Email: rasha.habeeb@coeng.uobaghdad.edu.iq

selectivity, energy efficiency, environmental compatibility, and adaptability [17]. Wastewater is treated with a variety of electrochemical techniques, such as electro-flotation, electro-Fenton, electrodialysis, electrocoagulation [18], and electro-oxidation [19, 20]

One of the most eco-friendly electrochemical approaches is the EC process which is known for its high adaptability and compatibility and approved for its high effectiveness in eliminating different toxic components from household and industrial wastewater [21-24] with low cost, low sludge production, and simple equipment requirements [7]. In the EC process, sacrificial anodes, which are often made of iron, nickel, or aluminum, would be dissolved by applying constant current or voltage over the electrolytic cell under controlled circumstances. Furthermore, water oxidation would take place at the anode resulting in O_2 gas production as shown in Eq. 1, and water reduction would take place at the cathode resulting in H_2 gas production as illustrated in Eq. 2 where these gases would enhance the flotation of generated flocs in the EC cell. Hydroxide ions (OH^-) would also be formed at the cathode from water reduction and reacted with metal ions to form metal hydroxides in the electrolytic solution which is considered the coagulant species which eliminates toxic components by neutralizing adsorption mechanism [24, 25].

$$H_2O \rightleftharpoons 4H^+_{(aq)} + O_{2(g)} + 4e^- \quad (1)$$

$$4H_2O + 4e^- \rightleftharpoons 2H_{2(g)} + 4HO^-_{(aq)} \quad (2)$$

By utilizing Al as the sacrificial anode, Al^{3+} ions would be produced and reacted with OH^- ions to form $Al(OH)_3$ as the main coagulants as shown in Eq. 3 [26, 27].

$$Al^{3+}_{aq} + 3OH^-_{aq} \leftrightarrow Al(OH)_3 \quad (3)$$

Ni is used properly as a current collector and is available in different forms and among these forms is lightweight Ni foam which is an efficient material due to its high porosity, high stability, and high capacitance [28]. The 3D structure of interwoven Ni metal would enhance its electrical and thermal conductivity and increase its resistance to corrosion [28]. When Ni anode dissolves, Ni^{2+} ions will be formed, their reaction with hydroxide ions will generate $Ni(OH)_2$ as illustrated in Eq. 4 [29].

$$Ni^{2+}_{(aq)} + 2OH^-_{(aq)} \rightarrow Ni(OH)_{2(s)} \quad (4)$$

Many previous studies illustrated that integrated or dual approaches would improve the overall removal of toxic components from wastewater by combining vital advantages of each method and lowering their disadvantages like high operating costs, chemical addition, and low removal efficiency. Furthermore, combining two approaches in wastewater treatment would enhance the flexibility in treating wastewater with various compositions due to possible fluctuations in the contaminant's load. One of the major goals of the present study is to combine the EC process with adsorption hence EC process is known for its effective destabilization of coagulants, while the adsorption process will provide adsorbents that can capture these particles due to their high surface area [30-32]

The combined utilization of EC and adsorption characterizes a promising approach for the comprehensive and efficient removal of a wide range of pollutants from wastewater. On the other hand, this combination will diminish the potential limitations of each method. For example, in an EC process if the concentration of pollutants is high this means that more current will be required to produce enough coagulants to remove these contaminants and consequently high consumed energy. While, in the adsorption approach, one of the main drawbacks is adsorbent saturation and the competitive effect of some contaminated components. Therefore, the dual approach can be a strategic solution to decrease their restrictions [31-33].

Increasing the potential of utilizing adsorbents with low-cost which may be wasted from different industries enhanced the opportunity for considering adsorption as one of the most attractive approaches for eliminating pollutants from wastewater. Usually, activated carbon is the most used adsorbent due to its high surface area and high porosity but its high price restricts its application. Consequently, the focus on discovering alternative low-cost adsorbents that may be made from natural materials or wastes was increased [33]

One of the low-cost and most commonly produced adsorbents is alum sludge which continuously builds up during the flocculation-clarification process in the systems of producing drinking water by utilizing alum coagulant and is subsequently eliminated from the liquid phase by sedimentation/filtration procedures [34]. Alum sludge disposal becomes a concern due to the high rate of its production as a result of the high rate of population growth and, consequently, the rising demand for drinking water. Therefore, more environmentally friendly and economically sustainable management of this sludge is preferred in the future [35]. Aluminum sulfate, or simply alum (Al_2 $(SO_4)_3.14H_2O$) is the most affordable and straightforward aluminum-based flocculent on the market that is utilized worldwide in the standard water treatment systems [36, 37]

Often, the produced sludge is disposed of in landfills or released straight into adjacent aquatic bodies which is not a suitable solution because of the opportunity for soil and water pollution from the chemical compounds employed in the drinking water treatment [38, 39]. Many Researchers paid a lot of attention lately to employing alum sludge in the adsorption matrix [40]; the microstructure of the solid waste is influenced by the calcination temperature, which could enhance the material's technical qualities [41]. Therefore, using waste alum sludge as a pre-treatment step for textile effluents containing reactive colors is an interesting study issue as it is a win-win approach for water treatment and waste management [42].

The primary goals of the present study are employing an integrated single reactor EC-Adsorption system that

combines the advantages of each process simultaneously and improving the 2D EC system with Ni foam and Aluminum anodes in removing MO dye by the addition of oven-dried alum sludge with different electrode arrangements. In addition, studying the effect of this combination on power consumption in the EC system in the presence of alum sludge as a low-cost adsorbent resulting from water purification plant effluents and investigating the possibility of waste management are one of the major goals. Adsorption isotherms and adsorption kinetics would be additionally investigated.

2- Experimental work

2.1. Chemicals

The chemicals in the present work were H_2SO_4 (Central Drug House (p) Ltd., India, 98% of purity), Hydrochloric acid (HCl) (Thomas Baker Pvt. Ltd., India, with 37% purity), Methyl Orange dye ($C_{14}H_{14}N_3NaO_3S$) (with a purity of 99.0 %, wave length= 464 nm, and molar mass= 327.33 g/mol), alum sludge waste from Karbala Water filtration station (Iraq), and NaCl (LOBA PVT Ltd., Mumbai India, with 99.5% purity). The utilized chemicals were of reagent grade and distilled water was used in the preparation of all aqueous solutions in accomplished chemicals, and Fig. 1 displays the structure of MO dye.

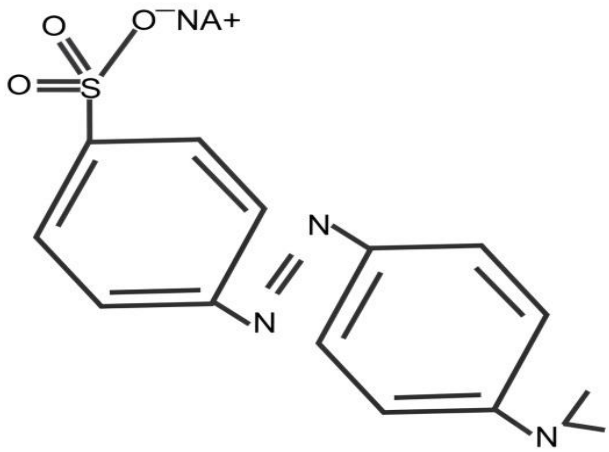

Fig. 1. The molecular structure of methyl orange dye

2.2. Alum sludge preparations and characterization

Dry alum sludge was collected from the Karbala-Iraq water purification plant. To form the sludge into the desired shape, a quantity of it was moisturized with distilled water to facilitate its formation and placed in a surgical needle. Cylindrical pieces were obtained with specified dimensions determined according to the required length and diameter of the particles. The average dimensions of the formed small pellets were 3.66 mm in diameter and (7- 9 mm) in length. Then they are dried before being prepared for use in experiments. A controlled heating within 24 hours at 105 °C for the small pellets was accomplished to ensure their drying and remove excess moisture and enhance its durability and stability. The result is a hardened substance, ready for further processing or application. Field emissive scanning electron microscopy (SEM, FEI-company), energy dispersive Spectroscopy (EDS, Bruker Company/Germany, with 100A, 25 kV and XFlash-6110), XRF Analyzers [X-ray Fluorescence Spectrometers] SPECTRO (model XEPOS, type 766004814), pore size and BET surface area were examined to detect the surface morphology and elements composition for the alum sludge and to measure the surface area of it before and after its utilization in the combined EC-Adsorption process. The Brunauer, Emmett, and Teller (BET) method is a technique used in practice to calculate the specific surface area which is based on the adsorption of liquid nitrogen at a constant temperature.

2.3. Dyes removal by EC-adsorption system

The batch experiments of the combined EC-Adsorption system were accomplished in a cubic glass cell (17 cm×17 cm×11 cm) and to maintain good mixing along experiments, this cell was placed onto a Heidolph magnetic stirrer (Germany) at a rotation speed of 250 rpm. The main anodes in these combined systems were either Ni foam (NiF), or Aluminum (Al), or both, while the cathodes were stainless steel (SS) mesh (type 316-AISI), and in all combined systems, the distance between any two electrodes was kept at 1.5 cm. The dimensions of each electrode were 6 cm in width and 14 cm in length, while the thickness of the Al, NiF, and SS mesh were 0.4, 1, and 0.1 cm, respectively. The electrodes were fixed in a vertical manner in the batch cell and the active area of one face of the anode was 39 cm^2.

It is worthy to declare that NiF, Al, and SS mesh electrodes were activated before each experiment to exclude impurities or oxide layers on their surface and this step was accomplished by submerging them into 1M of H_2SO_4 for NiF or HCl solution for Al and SS mesh within 10 minutes and then washed with distilled water. A DC power supply was used as the main source of electric power, and the applied current for each anode was observed with a digital multimeter. The electrolytic solution was prepared by using 2L of distilled water and the MO dye was added to maintain an initial concentration of 100 mg/L, and 1 g/L of NaCl was added as the main electrolytic in the solution to enhance its conductivity. Each experiment was conducted within 30 minutes of electrolysis. All experiments were accomplished at 25 ± 2°C, and in duplicate to confirm the reproducibility of the process, and the calculations of experimental results were assessed depending on the average values.

One of the most important factors influencing the efficiency of the EC and adsorption processes is the pH value [7]. Furthermore, according to earlier research, the pH range controls the ionic properties of dyes, the kinds of generated Al or NiF hydroxides, and, in turn, the mechanism of dye removal [43]. Since the results of several earlier research indicated that the best dye removal effectiveness was attained at neutral pH, the

experiments in this study were conducted at neutral pH (about 7) [7, 44].

Five combined systems were examined separately which had different configurations and different electrodes connections to detect which one would enhance the MO dye removal efficiency with the lowest residual of Ni ions if it was the main anode, hence the Ni is a very poisonous element. Therefore, these five combined systems were investigated at a current density of 4 mA/cm^2, in the presence of 1 g/L of NaCl and 10 g/L of Alum sludge, pH= 7, 100 mg/L of MO dye, and within 30 minutes of electrolysis.

Fig. 2 a illustrates the first combined system (S1) where one Ni foam was employed as anode and two SS mesh as cathodes, between each NiF side and each SS mesh cathode there was a SS net (6 cm× 14 cm× 1 cm) which is filled with alum sludge pellets and each face of this net would be polarized with the different charge from the opposite side of the faced electrode. System 2 (S2) is represented in Fig. 2 b which corresponds to S1 but uses Al plate instead of NiF as the main anode. System 3 (S3) as represented in Fig. 2 c used NiF as anode and two SS mesh as cathodes with alum sludge dispersed freely in the reactor. System 4 (S4) as represented in Fig. 2 d is the same as S3 but with Al plate as an anode instead of NiF. In the last System, System 5 (S5) as represented in Fig. 2 e, there are two anodes, one is NiF and the other is Al, and three SS mesh as cathodes which were placed among anodes, while the alum sludge dispersed freely in the reactor.

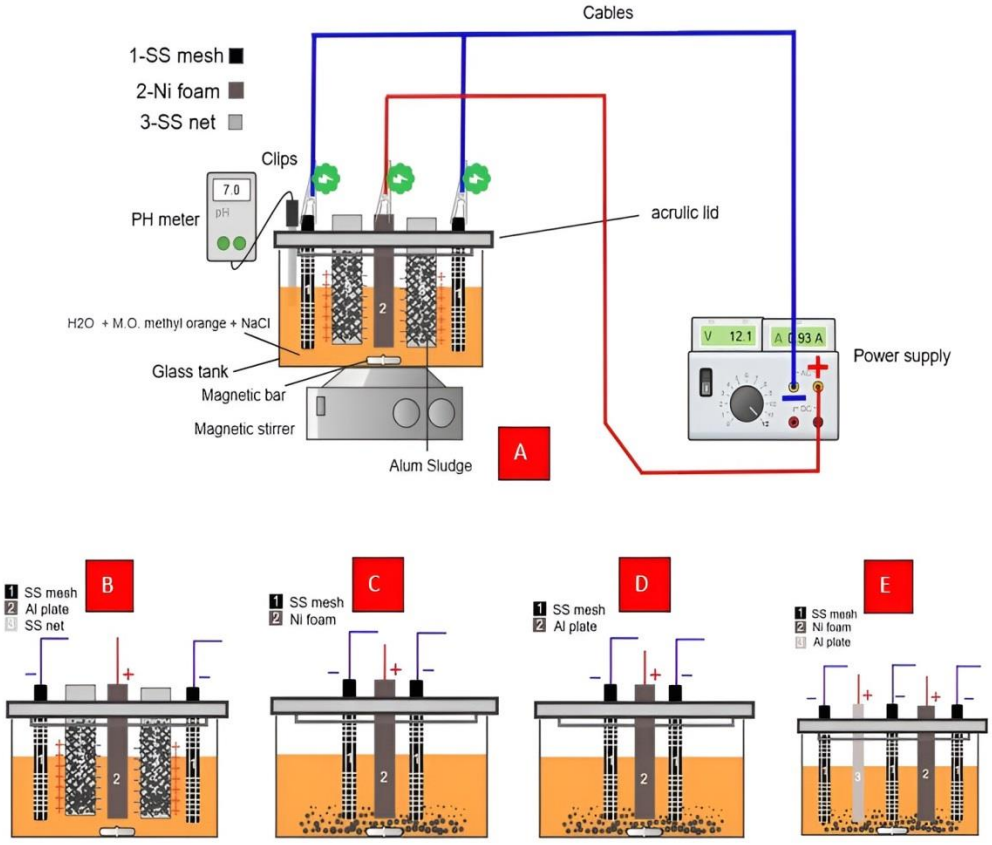

Fig. 2. EC-Adsorption combined systems; a: S1, b: S2, c: S3, d: S4, and e: S5

After detecting the best configuration from the five systems, it was worthy to explore the effect of different current densities on MO dye removal, which was studied at 4, 6, and 8 mA/cm^2, 1 g/l of NaCl, pH= 7, initial MO dye = 100 ppm, Alum sludge dosage = 10 g/l within 30 minutes. Furthermore, the effect of adsorbent loading was examined by adding 5, 10, and 20 g/L of alum sludge. Also, adsorption isotherms and kinetic calculations would be conducted as further work. To measure MO dye concentration in each sample before and after treatment, each sample would be analyzed with a UV–visible spectrophotometer (biotech Engineering Management CO. LTD, (UK) UV-9200). The calculation of MO dye concentration was based on the calibration curve at a maximum wavelength (λ_{max}) of 464 nm. The removal efficiency of MO dye is illustrated in Eq. 5 and to estimate the consumed energy (SEC) in (kWh/kg MO dye); Eq. 6 can be utilized [7, 45].

$$Methyl\ orange\ removal\ \% = \frac{(C_i - C_f)}{C_i} \times 100 \quad (5)$$

$$SEC = \frac{E \times I \times t}{(C_i - C_f) \times v} \times 1000 \quad (6)$$

Where: E is the voltage in (Volt), I is the applied current in (ampere), t is the electrolysis time in (h), v denotes the

volume of aqueous solution in (L), and C_i, C_f indicates the initial and final concentration of MO dye, respectively in mg/L.

To evaluate the adsorption capacity at equilibrium (q_e), Eq. 7 can be used [46]:

$$q_e = \frac{V(C_i - C_e)}{w} \quad (7)$$

Where: q_e is the adsorption capacity of the adsorbent (mg/g), V is the volume of the electrolytic solution (L), w is the weight of the consumed utilized anode (g), and C_i and C_e are the initial and equilibrium concentrations of adsorbate (MO dye), respectively (mg/L) [46].

3- Results and discussion

3.1. Detection of the best EC-adsorption combined system

Besides the basic two electrodes EC set-up, several electrodes can be connected in many possible forms within an EC cell to enhance removal efficiency and lower the consumed energy. In the systems S1 and S2, the anode (either NiF or Al) was connected to the positive while the two SS mesh cathodes were connected to the negative of the power source. Each face of the SS net would be polarized with a negative charge if it was opposite to the anode and with a positive charge if it was opposite to the cathode. The connection of electrodes in these two systems is a combination of parallel and series bipolar connections.

Based on the findings of many comparative previous studies, low-cost EC process can be predicted by applying a parallel electrode connection, while low maintenance and high removal efficiency can be obtained with the series bipolar connection [33, 47]. However, the EC optimum performance is governed by different operating conditions, contaminant types, and the wastewater medium, therefore these previous studies cannot be considered conclusive [33].

To investigate the effect of different electrode connections and arrangements on the MO dye removal efficiency and consumed energy; the five systems were studied under controlled conditions of 4 mA/cm^2, 1 g/L of NaCl, 10 g/L of Alum sludge, pH= 7, 100 mg/L of MO dye, and within 30 minutes of electrolysis. As shown in Fig. 3, it can be perceived that the MO dye removal percentage (Re%) for S1, S2, S3, S4, and S5 were 71.415, 42.138, 90.214, 33.138, and 81.691%, respectively. The highest removal efficiency of S3 can be established from the highest efficiency of NiF anode in comparison with Al anode due to its 3D structure which enhanced the mass transfer, and this was stated in our previous study [7]. In addition, the free alum sludge in aqueous solution enhanced the MO Re% in system S3 in comparison with S1 where it was fitted in the SS net and that can be revealed from the possibility of generated dead zone among the particles that included in the SS net in comparison with that surrounded with solution freely. S2 and S4 systems gave the lower MO Re% hence Al was the main anode, however connecting NiF and Al as the main parallel anodes in system S5 with alum sludge free in the solution gave better removal efficiency in comparison with S1, S2, and S4. The detection of the best combined system would be evaluated not on MO Re% basis but also on the basis of consumed energy in all systems. The SEC values for S1, S2, S3, S4, and S5 were estimated based on Eq. 6, the SEC were 36.96, 67.41, 31.58, 59.89, and 31.46 kWh/kg MO, respectively. As observed, S5 gave the lower value of consumed energy hence its connection is parallel, additionally, the systems S1 and S3 revealed low consumed energy because of the utilization of NiF as the anode in these systems, and this result is due to its 3D structure which enhances the electrical conductivity as mentioned previously resulting in lowering the voltage and in subsequent the consumed energy. As a result, the combined EC-Adsorption system S3 gave higher removal efficiency with low consumed energy.

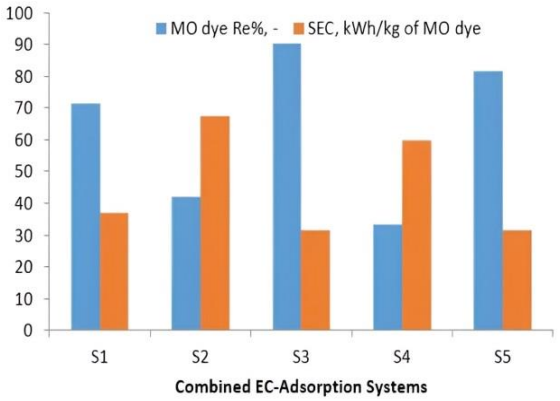

Fig. 3. Results of MO dye removal % with Different system Setups at 4 mA/cm^2, pH= 7, 100 mg/L of MO dye, NaCl conc. = 1 g/L, and 30 minutes of electrolysis

3.2. Effect of current density

The current density is actually one of the most significant operating factors that must be taken into account when designing any EC setup. It has a significant impact on the governing contaminant separation method in addition to the system response time. To prevent a decline in current efficiency and electrical energy waste, this crucial parameter must be managed [48, 49]

MO dye removal would be investigated for the five EC-Adsorption systems at three different current densities (4, 6, and 8 mA/cm^2), at 1 g/L of NaCl, pH = 7, initial MO dye concentration = 100 ppm, and alum sludge dose = 10 g/L within 30 minutes in order to determine each system's efficiency. Fig. 4, Fig. 5, and Fig. 6 illustrate the MO dye removal percentage at 4, 6, and 8 mA/cm^2, respectively. By examining these figures, not surprisingly; the MO dye removal % would increase by increasing the current density. By increasing the current density, more electrode ionic species (Ni^{2+} or Al^{3+}) would be generated from the anodes, resulting in increasing the production of $Ni(OH)_2$ or $Al(OH)_3$ flocs in the solution and, ultimately, the removal of MO dye would be increased. These results are in agreement with Faraday's law (m = [*ItM/zF*]).

Additionally, a higher current density would accelerate the formation of H_2 and O_2 gases, which has a significant effect on the electrodes' mass transfer, flotation, and solution mixing rates [7].

It can be detected from these figures that at 4 mA/cm^2, S3 followed by S5 and S1systems revealed the highest removal efficiency hence NiF was the main anode as in S1 and S3 systems or combined with Al anode as in S5 system. While S2 and S4 systems gave the lowest MO removal efficiency hence Al was the controlling anode. At 6 and 8 mA/cm^2, S3 followed by S1 and S5 systems gave the highest MO removal %. However, there is a simple enhancement in MO dye removal % as the current density increased from 6 to 8 mA/cm^2 as shown in Fig. 5 and Fig. 6. For example, in the S3 system, the MO dye removal % increased from 98.968 to 99.742% as the current density increased from 6 to 8 mA/cm^2.

In spite of excellent results by utilizing NiF as an anode as predicted from these results, it is worthy to remember that Ni metal is non-biodegradable and it is one of the most toxic heavy metals. Based on the World Health Organization (WHO) guidelines, the maximum allowable concentration of Ni in released industrial wastewater and drinking water is 2 and 0.1 mg/L, respectively [50].

Therefore, the detection of the best EC-Adsorption system is not governed by its efficiency in removing contaminants but consistently with that given the permissible concentration of Ni ions. The S3 system gave the highest MO dye removal efficiency at 8 mA/cm^2 but also with a high concentration of Ni which is equal to 4.2 mg/L, while at 6 mA/cm^2, it is 1.8 mg/L which can be considered within the limitations of WHO. Consequently, S3 can be operated at 6 mA/cm^2 to obtain 98.968% of MO dye removal efficiency with an allowable concentration of Ni ions.

2.4. Effect of alum sludge dosage

The adsorbent surface area and the amount of available binding sites are directly affected by the dosage of the adsorbent. The amount of contacting sorbent in the liquid phase is one of the factors that significantly influence the adsorption capacity since it establishes the adsorbent's capacity for a specific initial dye solution concentration [47, 51]. In the present study, three different dosages of alum sludge were tested in the combined S3 system with NiF as the anode hence it shows the highest MO dye removal efficiency with an acceptable amount of Ni ions with fixing other parameters as 30 minutes of treatment, 6 mA/cm^2 of current density, 1g/L of NaCl, pH = 7, initial concentration of MO dye = 100 mg/L, and the tested amounts of alum sludge were 5, 10, and 20 g/L. The results illustrated in Table 1 show that MO dye removal efficiency is not extremely influenced by increasing the amount of alum sludge but additionally, it can be concluded that it affects directly the amount of Ni ions that released in the treated solution due to NiF anode dissolution. By adding 5 g/L of alum sludge, 5.5 mg/L of Ni ions are presented in the solution which is not an acceptable value according to the WHO guidelines. Utilizing 10 g/L of alum sludge reduced the concentration of Ni ions to 1.8 mg/L which is considered acceptable to be released in aquatic bodies while increasing its quantity to 20 mg/L enhanced the removal of Ni ions to an acceptable value of 0.5 mg/L.

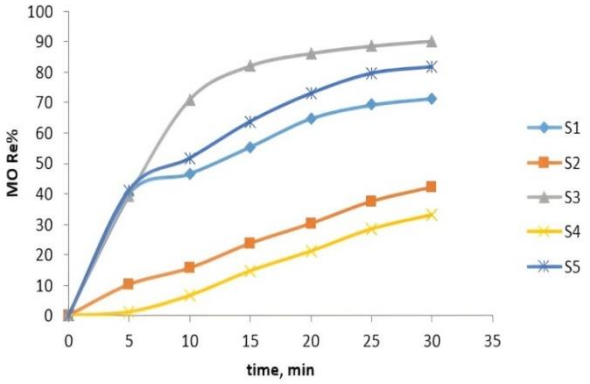

Fig. 4. MO dye removal % at 4 mA/cm^2, pH=7, 100 mg/L of MO dye, NaCl conc. = 1 g/L, 10 g/L of alum sludge, and 30 minutes of electrolysis

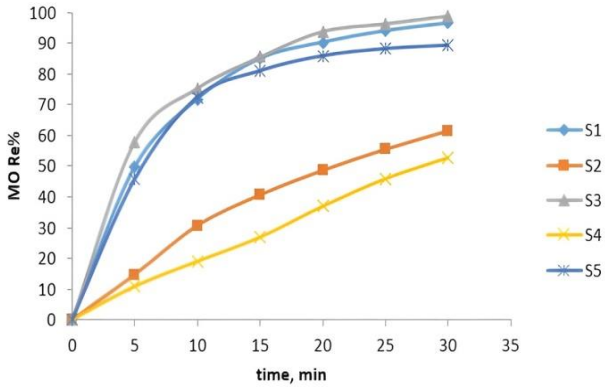

Fig. 5. MO dye removal % at 6 mA/cm^2, pH=7, 100 mg/L of MO dye, NaCl conc. = 1 g/L, 10 g/L of alum sludge, and 30 minutes of electrolysis

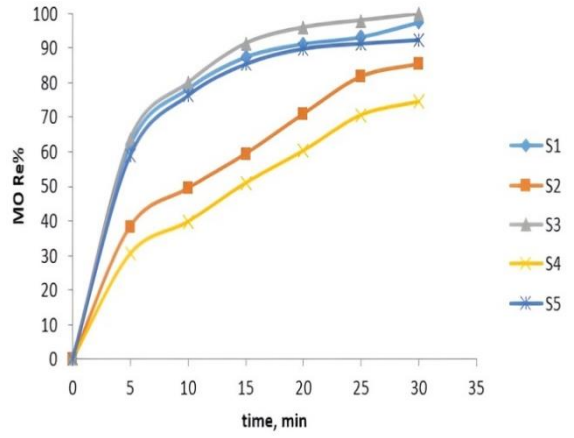

Fig. 6. MO dye removal % at 8 mA/cm^2, pH=7, 100 mg/L of MO dye, NaCl conc. = 1 g/L, 10 g/L of alum sludge, and 30 minutes of electrolysis

Table 1. Results of MO dye removal % and concentration of Ni ions at 6 mA/cm^2, pH=7, 100 mg/L of MO dye, NaCl conc. = 1 g/L, 30 minutes of electrolysis, and different alum sludge dosage

Alum sludge dosage, g/L	MO dye removal %	Nickel ions concentration, mg/L
5	98.17	5.5
10	98.54	1.8
20	98.74	0.5

2.5. Characterization of alum sludge

The EDS results for the alum sludge adsorbent before its utilization in the combined system are illustrated in Fig. 7. Fig. 7 indicated that O had the highest weight percentage of composition equal to 47.8% followed by carbon (21.05%) and the metal Si had the larger percentage of the total metals that naturally presented in alum sludge with 16.2% in addition to 5.5% of Al, 4.6% of Fe with minor components like Cr, Mg, Ti, Na, Cl, S, Ca, and K. After experiments, all alum sludge components were decreased hence there are many metals in its structure that can be dissolved under the effect of current to give their corresponding ions. The weight percentages of O, C, Si, Al, and Fe decreased to 43.58, 19.4, 13.38, 4.02, and 3.74%, respectively. Table 2 represents the XRF results which support the EDS results by providing further details on the metal hydroxides that make up the entire alum sludge.

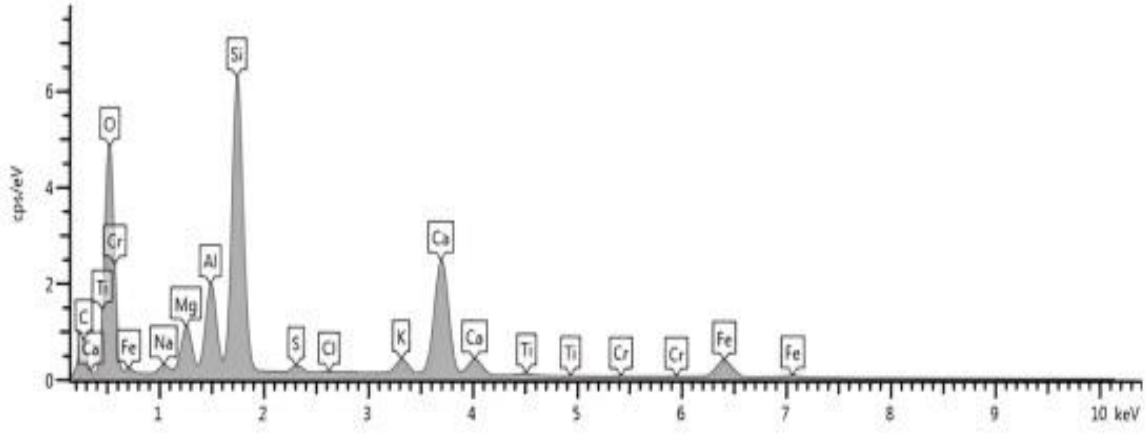

Fig. 7. EDS images of alum sludge

Table 2. XRF results of alum sludge

Compound	Na_2O	MgO	Al_2O_3	SiO_2	SO_3	K_2O	CaO	Fe_2O_3	MnO	TiO_2	Cr_2O_3	P_2O_5
Concentration, %	0.28	0.14	0.59	5.53	0.19	0.72	9.78	5.54	0.08	0.34	0.04	0.03

The morphological structure of alum sludge is shown in Fig. 8 prior to its utilization as an adsorbent in the EC-Adsorption combined system. A highly uneven and porous structure for alum sludge with agglomerates of different particle sizes is shown in Fig. 8. The surface is covered with small granular forms or micro-crystals, giving the texture a rough appearance. The adsorption of dye molecules is enhanced by high surface area and porosity. The physical stability of alum sludge makes regeneration and reuse possible. By decreasing waste disposal and increasing dye removal efficiency, the use of waste materials such as alum sludge in water treatment processes contributes to sustainability. The specific surface area (BET) and pore size for alum sludge were examined before and after experiments. It was found that the BET decreased from 26.995 to 19.5434 m^2/g as expected due to its saturation with contaminants, while pore size increased from 8.0381 to 9.29297 nm due to the increase in the agglomerations [52, 53].

2.6. Adsorption isotherms

Adsorption isotherm permits an estimation of the validity of applying an adsorbent and assessing its efficiency in adsorbing pollutants. It can be considered as one of the most useful ways to describe the interaction between the adsorbent and adsorbate at equilibrium state and determine the optimum adsorption capacity [54].

In addition, the analysis of experimental data after its fitting to various isotherms is considered a vital step to optimize the adsorbent properties and it helps in comprehending the mechanism of the adsorption process hence each isotherm model provides an evaluation of the certain physical and chemical properties required for the adsorption process [55]

In order to attain a detailed understanding of the adsorption of MO dye in the S3 EC-Adsorption combined system, the Langmuir and Freundlich isotherms have been applied in this study and these isotherms were evaluated based on their correlation coefficient (R^2) values. Langmuir adsorption isotherm as illustrated in Eq. 8 assumes a homogeneous surface energy distribution and adsorption takes place at specified homogeneous sites besides assuming monolayer adsorption [54, 56]

$$\frac{C_e}{q_e} = \frac{K_L}{q_m} + \frac{C_e}{q_m} \quad (8)$$

Where: q_m is the maximum adsorption capacity (mg/g) which is related to comprehensive monolayer coverage, K_L is the Langmuir constant, and it is consistent with the energy of adsorption (L/mg), C_e is the concentration of MO dye at equilibrium (mg/L). Fig. 9 shows a plot of $1/q_e$ versus $1/C_e$ to obtain a straight line where its slope and intercept would give the isotherm parameters and their values besides R^2 are listed in Table 3.

Freundlich model assumes non-uniform adsorption and with varying adsorption energy on adsorption surfaces [57]. Although it has been widely used in heterogeneous systems and can represent both multilayer and monolayer adsorption. It is criticized for not approaching Henry's law at low concentrations [56]. The foundation of the Freundlich multi-component isotherm is the idea that there is an exponential distribution of adsorption energies. Eq. 9 displays the model's linear form.

$$ln\, q_e = ln\, K_f + \frac{1}{n} ln\, C_e \quad (9)$$

Where: n is a constant related to the efficiency of sorption and sorption energy, K_f is the Freundlich constant (mg/g)/(mg/l)^1/n, n is the intensity of adsorption constant, and *Ce* is the equilibrium concentration of the adsorbate in solution [32] Fig. 9 displays a plot of ln q_e versus ln C_e to obtain a straight line where its slope and intercept would give the values of K_f and n, respectively besides R^2 which are listed in Table 3.

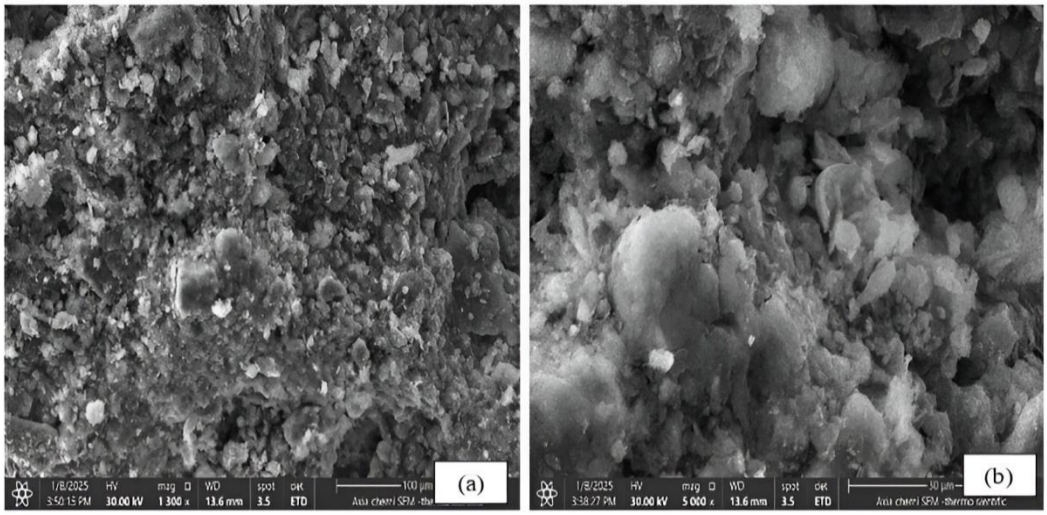

Fig. 8. FESEM images of alum sludge adsorbent before using at different magnifications ((a)100 µm, and (b) 30 µm)

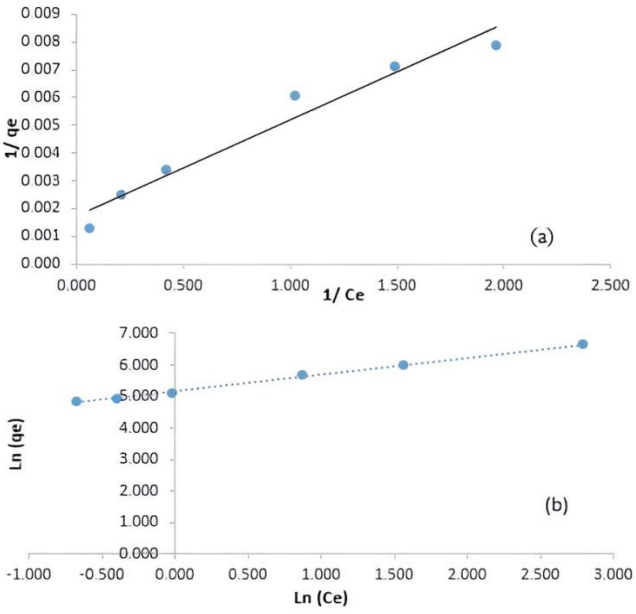

Fig. 9. a) Langmuir isotherm and b) Freundlich for MO dye removal at various current densities, initial MO dye concentration = 100 mg/L, pH = 7, NaCl concentration = 1 g/L, and 10 g/L of alum sludge

Table 3. Langmuir and Freundlich adsorption parameters

Langmuir isotherm results		Freundlich isotherm results	
Slope	0.0035	Slope	0.5322
Intercept	0.0017	Intercept	5.1682
R^2	0.9564	R^2	0.9974
q_m, (mg/g)	588.2352941	n	1.87899286
K_L, (1/mg)	0.485714286	K_f, (mg/g)/(mg/l) ^1/n	175.5984756

2.7. Adsorption kinetics

One of the vital factors that describe the effectiveness of sorption is its kinetics. The adsorption kinetics principally defines the reaction pathways, rate of adsorption for adsorbate, and the resident time of it on the solid-liquid boundary [54, 58]. There are two main resistances that take place during the adsorption process, the first one is the resistance to external diffusion, and the second is the intra-particle resistance [55]. The pseudo 1st-order, pseudo 2nd -order and intra-particle diffusion are some of the kinetic models that have been validated to define the adsorption rate by determining the process's rate constant which is essential to understand the dynamics of a specified adsorption issue [33, 55]

In this study, an analysis of the experimental data would be accomplished for the adsorption of MO dye in the S3 combined EC-Adsorption system at 6 mA/cm^2, pH = 7, NaCl concentration = 1g/L, alum sludge dosage = 10 g/L by applying the simple linear equation of pseudo 1st-order Eq. 10, pseudo 2nd-order Eq. 11, and intra-particle diffusion Eq. 12 models to define the rate and mechanism of the adsorption of adsorbate by the adsorbent [33, 59].

$$\ln(q_e - q_t) = \ln q_e - k_1 t \quad (10)$$

$$\frac{t}{q_t} = \frac{1}{k_2 q_e^2} + \frac{1}{q_e}(t) \quad (11)$$

$$q_t = k_3 t^{0.5} + C \quad (12)$$

Where: q_t is the adsorption capacity of the adsorbent (mg/g) at time t (min), k_1 (min^{-1}), k_2 (g/ (mg.min)), and k_3 (mg/ (g. min$^{0.5}$)) are the rate constant for pseudo 1st-order, pseudo 2nd-order, and intra-particle diffusion models, respectively, and C (mg/g) is the thickness of the boundary layer [32]

By plotting ln(q_e-q_t) versus time, the values of k_1 and q_e can be determined from the slope and intercept, respectively as shown in Fig. 10a.

However, the pseudo 2nd-order assumes that there is a direct proportionality between the rate constant with the available active sites of adsorbents. The chemisorption kinetics of MO dye and the adsorbent can be examined by applying this kinetic model [55]. Fig. 10b illustrates the results of applying this kinetic model. Fig. 10c shows the results of applying intra-particle diffusion model by plotting q_t versus $t^{0.5}$ where k_3 is the slope and C is the intercept of the straight line.

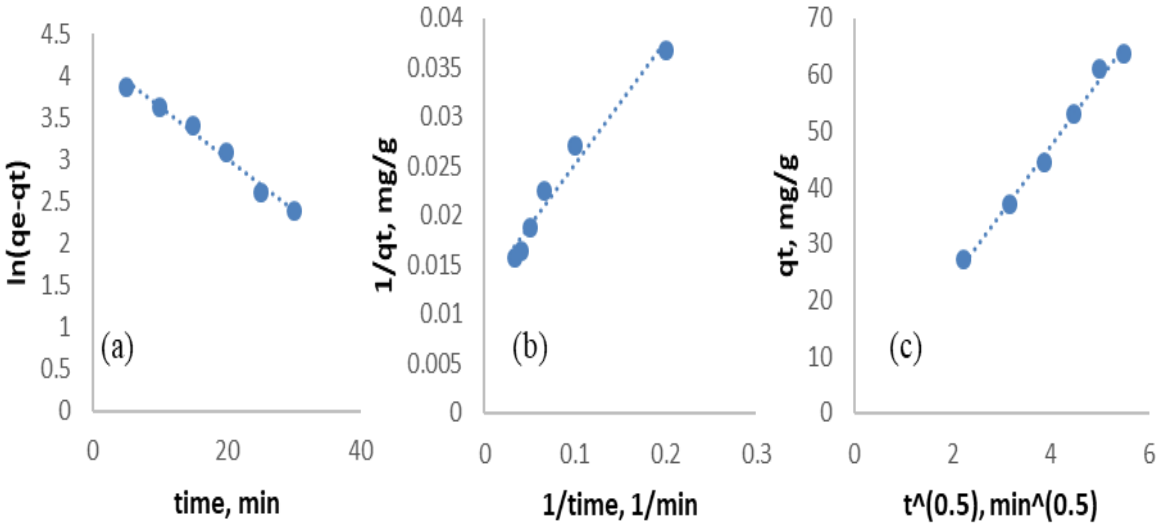

Fig. 10. a) Pseudo 1st –order, b) Pseudo 2nd –order, and c) intra-particle diffusion plots for MO dye removal at 6 mA/cm^2, initial MO dye concentration = 100 mg/L, pH = 7, NaCl concentration = 1g/L, alum sludge dosage = 10 g/L

Fig. 10 and the kinetic parameters illustrated in Table 4 state that practically alum sludge and Ni hydroxides have greater linear regression coefficients (R^2) in intra-particle diffusion model than in pseudo 1st -order kinetic and pseudo 2nd-order kinetic models. These results identify that the adsorption process in this combined system is a multiple adsorption process hence C ≠ 0 and the line did not pass through the origin point (0,0) and the intra-particle diffusion kinetic is not the only rate-limiting step and the value of C states the extent of boundary layer thickness [59].

Table 4. Kinetic parameters of pseudo 1st –order, pseudo 2nd –order, and intra-particle diffusion models

Kinetic Model	Kinetic Parameters	Parameters value
pseudo 1st-order	k_1, (min^{-1})	0.0615
	q_e, (mg/g)	69.44950905
	R^2	0.984
pseudo 2nd-order	k_2, (g/ (mg.min))	50030.30836
	q_e, (mg/g)	79.36507937
	R^2	0.9694
intra-particle diffusion	k_3, (mg/ (g. min0.5))	11.818
	C, (mg/g)	0.0642
	R^2	0.9925

4- Conclusion

The main goal of this study was to predict the efficiency of five EC-Adsorption systems which have different configurations with the utilization of alum sludge as a low-cost waste as adsorbent. This waste is rejected with high rates as a result of coagulation step through the process of drinking water treatment. The removal of MO dye by these combined systems was examined and it was concluded that systems with NiF anode were most effective than systems with Al as anode and alum sludge loaded freely in aqueous solution was better than loading it into SS nets. The combined system S3 showed the highest removal efficiency besides low concentrations of released Ni ions. The results also showed that MO dye removal % increased by increasing current density. However, there was a very small difference in the MO dye removal percentage as the current density increased from 6 to 8 mA/cm^2 besides that higher value of current densities means higher values of consumed energy and leached Ni ions. The alum sludge dosage enhanced the MO dye removal with minor rate, but it reduced the quantity of leached Ni ions to acceptable values. The adsorption kinetics of MO removal in the EC-Adsorption combined system referred as S3 followed the intra-particle diffusion model and the value of C confirmed that there was a multiple adsorption, and the Freundlich isotherm better fitted the experimental adsorption results based on its highest value of the correlation coefficient (R^2). The utilization of alum sludge with EC system enhanced the removal of MO dye and reduced the excess of released nickel in the solution which make it a great option for an environmentally friendly EC system.

References

[1] M. Anwar-ul-Haq, A.J. Hashmat, E. Islam, M. Afzal, A. Mahmood, M. Ibrahim, M. Nawaz, S. Nadeem, Q.M. Khan, "Pilot-Scale Electrochemical Treatment of Textile Effluent and its Toxicological Assessment for Tilapia (Oreochromis niloticus L.) Culture," *Pakistan Journal of Zoology*, vol. 50, no. 5, 2018, https://doi.org/10.17582/journal.pjz/2018.50.4.1703.1708

[2] S. Khelifi, A. Choukchou-Braham, H. M. Sbihi, M. Azam, S. I. Al-Resayes, and F. Ayari, "Treatment of textile dyeing wastewater using advanced photo-oxidation processes for decolorization and cod reduction," *Desalination and Water Treatment*, vol. 217, pp. 350–357, 2021, https://doi.org/10.5004/dwt.2021.26895

[3] H. Q. Ali and A. A. Mohammed, "Elimination of Congo Red Dyes From Aqueous Solution Using Eichhornia Crassipes," *Iraqi Journal of Chemical and Petroleum Engineering*, vol. 21, no. 4, pp. 21–32, Dec. 2020, https://doi.org/10.31699/ijcpe.2020.4.3

[4] T. A. Aragaw, "Potential and prospects of reductases in azo dye degradation: a review," *The Microbe*, vol. 4, p. 100162, Sep. 2024, https://doi.org/10.1016/j.microb.2024.100162

[5] A. Yaqub, H. Raza, H. Ajab, S. H. Shah, A. Shad, and Z. A. Bhatti, "Decolorization of reactive blue-2 dye in aqueous solution by electrocoagulation process using aluminum and steel electrodes," *Journal of Hazardous Materials Advances*, vol. 9, p. 100248, Feb. 2023, https://doi.org/10.1016/j.hazadv.2023.100248

[6] I. Louati *et al.*, "Simultaneous cleanup of Reactive Black 5 and cadmium by a desert soil bacterium," *Ecotoxicology and Environmental Safety*, vol. 190, Mar. 2020, https://doi.org/10.1016/j.ecoenv.2019.110103

[7] A. T. Mohammed Ali and R. H. Salman, "Enhancing the Removal of Methyl Orange Dye by Electrocoagulation System with Nickel Foam Electrode – Optimization with Surface Response Methodology," *Journal of Ecological Engineering*, vol. 25, no. 12, pp. 26–38, 2024, https://doi.org/10.12911/22998993/193587

[8] S. M. Alardhi, S. S. Fiyadh, A. D. Salman, and M. Adelikhah, "Prediction of methyl orange dye (MO) adsorption using activated carbon with an artificial neural network optimization modeling," *Heliyon*, vol. 9, no. 1, Jan. 2023, https://doi.org/10.1016/j.heliyon.2023.e12888

[9] R. Al-Tohamy, S.S. *Ali, F. Li, K.M. Okasha, Y.A.G. Mahmoud, T. Elsamahy, H. Jiao, Y. Fu, J. Sun*, "A critical review on the treatment of dye-containing wastewater: Ecotoxicological and health concerns of textile dyes and possible remediation approaches for environmental safety," *Ecotoxicology and Environmental Safety*, Feb. 01, 2022, https://doi.org/10.1016/j.ecoenv.2021.113160

[10] Q. Ye, H. Wu, J. Li, Y. Huang, M. Zhang, Q. Yi, B. Yan, "Preparation of 1,8-dichloroanthraquinone/graphene oxide/poly (vinylidene fluoride) (1,8-AQ/GO/PVDF) mediator membrane and its application to catalyzing biodegradation of azo dyes," *Ecotoxicology and Environmental Safety*, vol. 268, Dec. 2023, https://doi.org/10.1016/j.ecoenv.2023.115681

[11] N. Jawad and T. M. Naife, "Mathematical Modeling and Kinetics of Removing Metal Ions from Industrial Wastewater," *Iraqi Journal of Chemical and Petroleum Engineering*, vol. 23, no. 4, pp. 59–69, Dec. 2022, https://doi.org/10.31699/ijcpe.2022.4.8

[12] P. Moradihamedani, "Recent advances in dye removal from wastewater by membrane technology: a review," *Polymer Bulletin*, Apr. 01, 2022, https://doi.org/10.1007/s00289-021-03603-2

[13] J. Joseph, R. C. Radhakrishnan, J. K. Johnson, S. P. Joy, and J. Thomas, "Ion-exchange mediated removal of cationic dye-stuffs from water using ammonium phosphomolybdate," *Materials Chemistry and Physics*, vol. 242, Feb. 2020, https://doi.org/10.1016/j.matchemphys.2019.122488

[14] Y. N. Teixeira, F. J. de Paula Filho, V. P. Bacurau, J. M. C. Menezes, A. Zhong Fan, and R. P. F. Melo, "Removal of Methylene Blue from a synthetic effluent by ionic flocculation," *Heliyon*, vol. 8, no. 10, Oct. 2022, https://doi.org/10.1016/j.heliyon.2022.e10868

[15] C. Zaharia, C. P. Musteret, and M. A. Afrasinei, "The Use of Coagulation–Flocculation for Industrial Colored Wastewater Treatment—(I) The Application of Hybrid Materials," *Applied Sciences*, Mar. 01, 2024, https://doi.org/10.3390/app14052184

[16] Ö. Gökkuş, E. Brillas, and I. Sirés, "Sequential use of a continuous-flow electrocoagulation reactor and a (photo)electro-Fenton recirculation system for the treatment of Acid Brown 14 diazo dye," *Science of the Total Environment*, vol. 912, Feb. 2024, https://doi.org/10.1016/j.scitotenv.2023.169143

[17] R. N. Abbas and A. S. Abbas, "Kinetics and Energetic Parameters Study of Phenol Removal from Aqueous Solution by Electro-Fenton Advanced Oxidation Using Modified Electrodes with PbO2 and Graphene," *Iraqi Journal of Chemical and Petroleum Engineering*, vol. 23, no. 2, pp. 1–8, Jun. 2022, https://doi.org/10.31699/ijcpe.2022.2.1

[18] Q. H. Nguyen, T. *Watari, T. Yamaguchi, Y. Takimoto, K. Niihara, J.P. Wiff, T. Nakayama*, "COD removal from artificial wastewater by electrocoagulation using aluminum electrodes," *International Journal of Electrochemical Science*, vol. 15, no. 1, pp. 39–51, Jan. 2020, https://doi.org/10.20964/2020.01.42

[19] P. V. Nidheesh, M. Zhou, and M. A. Oturan, "An overview on the removal of synthetic dyes from water by electrochemical advanced oxidation processes," *Chemosphere*, vol. 197, pp. 210–227, Apr. 2018, https://doi.org/10.1016/j.chemosphere.2017.12.195

[20] H. J. Nsaif, N. S. Majeed, and R. H. Salman, "Preparation of nano SnO2-Sb2O3composite electrode by cathodic deposition for the elimination of phenol by Sonoelectrochemical oxidation," *Polish Journal of Chemical Technology*, Sep. 2024, https://doi.org/10.2478/pjct-2024-0026

[21] S. H. Ammar, N. N. Ismail, A. D. Ali, and W. M. Abbas, "Electrocoagulation technique for refinery wastewater treatment in an internal loop split-plate airlift reactor," *Journal of Environmental Chemical Engineering*, vol. 7, no. 6, Dec. 2019, https://doi.org/10.1016/j.jece.2019.103489

[22] T. Kim, T. K. Kim, and K. D. Zoh, "Removal mechanism of heavy metal (Cu, Ni, Zn, and Cr) in the presence of cyanide during electrocoagulation using Fe and Al electrodes," *Journal of Water Process Engineering*, vol. 33, Feb. 2020, https://doi.org/10.1016/j.jwpe.2019.101109

[23] J. Liu, W. Jiang, G. Wang, L. Zhang, Y. Chen, and R. Xin, "Experimental study on removal of emulsified oil by electrocoagulation with a rotating container," *International Journal of Electrochemical Science*, vol. 14, no. 6, pp. 5122–5131, Jun. 2019, https://doi.org/10.20964/2019.06.47

[24] K. Gautam, S. Kamsonlian, and S. Kumar, "Removal of Reactive Red 120 dye from wastewater using electrocoagulation: optimization using multivariate approach, economic analysis, and sludge characterization," *Separation Science and Technology (Philadelphia)*, vol. 55, no. 18, pp. 3412–3426, Dec. 2020, https://doi.org/10.1080/01496395.2019.1677713

[25] T. Jovanović, N. *Velinov, M. Petrović, S. Najdanović, D. Bojić, M. Radović, A. Bojić,* "Mechanism of the electrocoagulation process and its application for treatment of wastewater: A review," *Advanced Technologies*, vol. 10, no. 1, pp. 63–72, 2021, https://doi.org/10.5937/savteh2101063j

[26] Y. J. Liu, S. L. Lo, Y. H. Liou, and C. Y. Hu, "Removal of nonsteroidal anti-inflammatory drugs (NSAIDs) by electrocoagulation-flotation with a cationic surfactant," *Separation and Purification Technology*, vol. 152, pp. 148–154, Aug. 2015, https://doi.org/10.1016/j.seppur.2015.08.015

[27] S. C. M. Signorelli, J. M. Costa, and A. F. de Almeida Neto, "Electrocoagulation-flotation for orange II dye removal: Kinetics, costs, and process variables effects," *Journal of Environmental Chemical Engineering*, vol. 9, no. 5, Oct. 2021, https://doi.org/10.1016/j.jece.2021.106157

[28] N. A. Salleh, S. Kheawhom, and A. A. Mohamad, "Characterizations of nickel mesh and nickel foam current collectors for supercapacitor application," *Arabian Journal of Chemistry*, vol. 13, no. 8, pp. 6838–6846, Aug. 2020, https://doi.org/10.1016/j.arabjc.2020.06.036

[29] K. Muthumanickam and R. Saravanathamizhan, "Electrochemical treatment of dye wastewater using nickel foam electrode," *Journal of Electrochemical Science and Engineering*, vol. 11, no. 3, pp. 209–215, 2021, https://doi.org/10.5599/jese.1011

[30] H. H. Thwaini and R. H. Salman, "Modification of Electro-Fenton Process with Granular Activated Carbon for Phenol Degradation – Optimization by Response Surface Methodology," *Journal of Ecological Engineering*, vol. 24, no. 9, pp. 92–104, 2023, https://doi.org/10.12911/22998993/168411

[31] F. Sher, S.Z. *Iqbal, T. Rasheed, K. Hanif, J. Sulejmanović, F. Zafar, E.C. Lima,* "Coupling of electrocoagulation and powder activated carbon for the treatment of sustainable wastewater," *Environmental Science and Pollution Research*, vol. 28, no. 35, pp. 48505–48516, Sep. 2021, https://doi.org/10.1007/s11356-021-14129-5

[32] P. Twizerimana and Y. Wu, "Overview of integrated electrocoagulation-adsorption strategies for the removal of heavy metal pollutants from wastewater," *Discover Chemical Engineering*, vol. 4, no. 1, Jun. 2024, https://doi.org/10.1007/s43938-024-00053-w

[33] N. S. Graça and A. E. Rodrigues, "The Combined Implementation of Electrocoagulation and Adsorption Processes for the Treatment of Wastewaters," *Clean Technologies*, Dec. 01, 2022, https://doi.org/10.3390/cleantechnol4040063

[34] M. A. Tantawy, "Characterization and pozzolanic properties of calcined alum sludge," *Materials Research Bulletin*, vol. 61, pp. 415–421, 2015, https://doi.org/10.1016/j.materresbull.2014.10.042

[35] R. Liu, Y. Zhao, C. Sibille, and B. Ren, "Evaluation of natural organic matter release from alum sludge reuse in wastewater treatment and its role in P adsorption," *Chemical Engineering Journal*, vol. 302, pp. 120–127, Oct. 2016, https://doi.org/10.1016/j.cej.2016.05.019

[36] Y. Yang, Y. Zhao, R. Liu, and D. Morgan, "Global development of various emerged substrates utilized in constructed wetlands," *Bioresource Technology*, Aug. 01, 2018, *Elsevier Ltd*. https://doi.org/10.1016/j.biortech.2018.03.085

[37] N. Muisa, I. Nhapi, W. Ruziwa, and M. M. Manyuchi, "Utilization of alum sludge as adsorbent for phosphorus removal in municipal wastewater: A review," *Journal of Water Process Engineering*, Jun. 01, 2020, *Elsevier Ltd*. https://doi.org/10.1016/j.jwpe.2020.101187

[38] T. Ahmad, K. Ahmad, and M. Alam, "Characterization of Water Treatment Plant's Sludge and its Safe Disposal Options," *Procedia Environmental Sciences*, vol. 35, pp. 950–955, 2016, https://doi.org/10.1016/j.proenv.2016.07.088

[39] P. Devi and A. K. Saroha, "Utilization of sludge based adsorbents for the removal of various pollutants: A review," *Science of The Total Environment*, Feb. 01, 2017, *Elsevier B.V.* https://doi.org/10.1016/j.scitotenv.2016.10.220

[40] Q. Hou, P. Meng, H. Pei, W. Hu, and Y. Chen, "Phosphorus adsorption characteristics of alum sludge: Adsorption capacity and the forms of phosphorus retained in alum sludge," *Materials Letters*, vol. 229, pp. 31–35, Oct. 2018, https://doi.org/10.1016/j.matlet.2018.06.102

[41] M. Kasina, M. Wendorff-Belon, P. R. Kowalski, and M. Michalik, "Characterization of incineration residues from wastewater treatment plant in Polish city: a future waste based source of valuable elements?," *Journal of Material Cycles and Waste Management*, vol. 21, no. 4, pp. 885–896, Jul. 2019, https://doi.org/10.1007/s10163-019-00845-1

[42] M. A. Tony, "Zeolite-based adsorbent from alum sludge residue for textile wastewater treatment," *International Journal of Environmental Science and Technology*, vol. 17, no. 5, pp. 2485–2498, May 2020, https://doi.org/10.1007/s13762-020-02646-8

[43] F. Benaissa, H. Kermet-Said, and N. Moulai-Mostefa, "Optimization and kinetic modeling of electrocoagulation treatment of dairy wastewater," *Desalination Water Treat*, vol. 57, no. 13, pp. 5988–5994, Mar. 2016, https://doi.org/10.1080/19443994.2014.985722

[44] Y. Liu, C. Li, J. Bao, X. Wang, W. Yu, and L. Shao, "Degradation of Azo Dyes with Different Functional Groups in Simulated Wastewater by Electrocoagulation," *Water (Switzerland)*, vol. 14, no. 1, Jan. 2022, https://doi.org/10.3390/w14010123

[45] A. Abbas Najim and A. A. Mohammed, "Biosorption of Methylene Blue from Aqueous Solution Using Mixed Algae," *Iraqi Journal of Chemical and Petroleum Engineering*, vol. 19, no. 4, pp. 1–11, Dec. 2018, https://doi.org/10.31699/ijcpe.2018.4.1

[46] G. S. Aljeddani, R. M. Alghanmi, and R. A. Hamouda, "Study on the Isotherms, Kinetics, and Thermodynamics of Adsorption of Crystal Violet Dye Using Ag-NPs-Loaded Cellulose Derived from Peanut-Husk Agro-Waste," *Polymers (Basel)*, vol. 15, no. 22, Nov. 2023, https://doi.org/10.3390/polym15224394

[47] P. Twizerimana and Y. Wu, "Overview of integrated electrocoagulation-adsorption strategies for the removal of heavy metal pollutants from wastewater," *Discover Chemical Engineering*, vol. 4, no. 1, Jun. 2024, https://doi.org/10.1007/s43938-024-00053-w

[48] S. Irki, D. Ghernaout, and M. W. Naceur, "Decolourization of methyl orange (MO) by electrocoagulation (EC) using iron electrodes under a magnetic field (MF)," *Desalination and Water Treatment*, vol. 79, pp. 368–377, Jun. 2017, https://doi.org/10.5004/dwt.2017.20797

[49] M. Kul, K.O. *Oskay, F. Erden, E. Akça, R. Katirci, E. Köksal, E., Akinci,* "Effect of process parameters on the electrodeposition of zinc on 1010 Steel: Central composite design optimization," *International Journal of Electrochemical Science*, vol. 15, pp. 9779–9795, 2020, https://doi.org/10.20964/2020.10.19

[50] H. N. M. Ekramul Mahmud, A. K. Obidul Huq, and R. B. Yahya, "The removal of heavy metal ions from wastewater/aqueous solution using polypyrrole-based adsorbents: A review," *RSC Advances*, 2016, https://doi.org/10.1039/c5ra24358k

[51] A. M. Aljeboree, A. F. Alkaim, and A. H. Al-Dujaili, "Adsorption isotherm, kinetic modeling and thermodynamics of crystal violet dye on coconut husk-based activated carbon," *Desalination and Water Treatment*, vol. 53, no. 13, pp. 3656–3667, Mar. 2015, https://doi.org/10.1080/19443994.2013.877854

[52] K. O. Iwuozor, J. O. Ighalo, E. Chizitere Emenike, C. Adaobi Igwegbe, and A. G. Adeniyi, "Do adsorbent pore size and specific surface area affect the kinetics of methyl orange aqueous phase adsorption?," *Journal of Chemistry Letters*, vol. 2, pp. 188–198, 2021, https://doi.org/10.22034/JCHEMLETT.2022.327407.1048

[53] M. Sabharwal and M. Secanell, "Understanding the effect of porosity and pore size distribution on low loading catalyst layers," *Electrochimica Acta*, vol. 419, Jul. 2022, https://doi.org/10.1016/j.electacta.2022.140410

[54] M. Musah, Y. Azeh, J. Mathew, M. Umar, Z. Abdulhamid, and A. Muhammad, "Adsorption Kinetics and Isotherm Models: A Review," *Caliphate Journal of Science and Technology*, vol. 4, no. 1, pp. 20–26, Feb. 2022, https://doi.org/10.4314/cajost.v4i1.3

[55] S. I. Al-Saeedi, A. *Areej, M.T. Qamar, A. Alhujaily, S. Iqbal, M.T. Alotaibi, M. Aslam, M.A. Qayyum, A., Bahadur, N.S. Awwad, Y. Jazaa, E.B. Elkaeed*, "Isotherm and kinetic studies for the adsorption of methylene blue onto a novel Mn3O4-Bi2O3 composite and their antifungal performance," *Frontiers in Environmental Science*, vol. 11, 2023, https://doi.org/10.3389/fenvs.2023.1156475

[56] K. A. Babatunde, B. M. Negash, S. R. Jufar, T. Y. Ahmed, and M. R. Mojid, "Adsorption of gases on heterogeneous shale surfaces: A review," *Journal of Petroleum Science and Engineering*, Jan. 01, 2022, *Elsevier B.V.* https://doi.org/10.1016/j.petrol.2021.109466

[57] Y. Wang, Y. Zhu, S. Liu, and R. Zhang, "Pore characterization and its impact on methane adsorption capacity for organic-rich marine shales," *Fuel*, vol. 181, pp. 227–237, Oct. 2016, https://doi.org/10.1016/j.fuel.2016.04.082

[58] S. Mustapha, D.T. *Shuaib, M.M. Ndamitso, M.B. Etsuyankpa, A. Sumaila, U.M. Mohammed, M.B., Nasirudeen*, "Adsorption isotherm, kinetic and thermodynamic studies for the removal of Pb(II), Cd(II), Zn(II) and Cu(II) ions from aqueous solutions using Albizia lebbeck pods," *Applied Water Science*, vol. 9, no. 6, Aug. 2019, https://doi.org/10.1007/s13201-019-1021-x

[59] G. S. Aljeddani, R. M. Alghanmi, and R. A. Hamouda, "Study on the Isotherms, Kinetics, and Thermodynamics of Adsorption of Crystal Violet Dye Using Ag-NPs-Loaded Cellulose Derived from Peanut-Husk Agro-Waste," *Polymers (Basel)*, vol. 15, no. 22, Nov. 2023, https://doi.org/10.3390/polym15224394

تحسين إزالة صبغة الميثيل البرتقالي عن طريق الجمع بين نظام التخثير الكهربائي وعملية الامتزاز بواسطة حمأة الشب المجففة بالفرن: اعتماد أنظمة مركبة مختلفة

آمور طلال محمد علي [١]، رشا حبيب سلمان [١،*]

١ قسم الهندسة الكيمياوية، كلية الهندسة، جامعة بغداد، بغداد، العراق

الخلاصة

نظرًا لخصائصها المقاومة، تُعدّ أصباغ الآزو، مثل الميثيل البرتقالي (MO)، مواد شديدة السمية، مما يجعل إزالتها من مياه الصرف الصحي لصناعة النسيج مشكلةً كبيرة. باستخدام تكوينات مختلفة لأنظمة التخثير الكهربائي–الامتزاز المدمجة، وإعادة استخدام حمأة الشب كمادة ممتزة، تسعى الدراسة الحالية إلى دراسة كفاءة هذه الأنظمة المختلفة في إزالة صبغة الميثيل البرتقالي. ولتقدير فوائدها وعيوبها، أُجريت تجارب باستخدام لوح فوم النيكل (NiF) ولوح الألومنيوم (Al) كأقطاب موجبة، وشبكة من الفولاذ المقاوم للصدأ (SS) كأقطاب سالبة، بوجود حمأة الشب كمادة ممتزة في جميع الأنظمة. حقق نظام التخثير الكهربائي–الامتزاز المركب، الذي يضم فلوريد النيكل (NiF) كأنود وشبكتين من الفولاذ المقاوم للصدأ (SS) ككاثودات، بتركيز ١٠ جم/لتر من حمأة الشب في المحلول، والمشار إليه بالنظام S3، كفاءة إزالة لصبغة MO بنسبة ٩٨,٩٦٨% خلال ٣٠ دقيقة دون الحاجة إلى معالجة مطولة، وبتركيز منخفض جدًا من أيونات النيكل الموجودة في المحلول المعالج. تضمنتت الدراسة كذلك قياس للمساحة السطحية (BET)، وحجم المسام (pore size)، وشكل السطح، والتركيب لحمأة الشب. وقد عزز استخدام حمأة الشب في النظام المركب إزالة أيونات النيكل الزائدة، وقلل من تأثيرها في المحاليل المعالجة، وعزز كفاءة إزالة صبغة MO بشكل قليل. لفهم حركية التفاعل و الأمتزاز طبقت عدة موديلات و وجد أنه امتزاز صبغة MO في نظام المركب المشار له بالنظام S3 يتبع موديل حركية التفاعل intra–particle diffusion، وموديل Freundlich وصف الية الأمتزاز.

الكلمات الدالة: أنظمة مركبة، أطيان الشب، التخثر الكهربائي، الامتزاز، النموذج الحركي ، صبغة المثيل البرتقالية.